Macroscopic Ionic Flow in a Superionic Conductor Na^+ β-Alumina Driven by Single-Cycle Terahertz Pulses

Yasuo Minami,[1,2,*] Benjamin Ofori-Okai,[3] Prasahnt Sivarajah,[3] Ikufumi Katayama,[2] Jun Takeda,[2] Keith A. Nelson,[3] and Tohru Suemoto[4]

[1]*Department of Industrial and Social Sciences, Tokushima University, Tokushima 770-8506, Japan*
[2]*Department of Physics, Faculty of Engineering Science, Yokohama National University, Yokohama 240-8501, Japan*
[3]*Department of Chemistry, Massachusetts Institute of Technology, Massachusetts 02139, USA*
[4]*Toyota Physical and Chemical Research Institute, Nagakute, Aichi 480-1192, Japan*

(Received 31 January 2020; accepted 28 February 2020; published 9 April 2020)

Ionic motion significantly contributes to conductivity in devices such as memory, switches, and rechargeable batteries. In our work, we experimentally demonstrate that intense terahertz electric-field transients can be used to manipulate ions in a superionic conductor, namely Na^+ β-alumina. The cations trapped in the local potential minima are accelerated using single-cycle terahertz pulses, thereby inducing a macroscopic current flow on a subpicosecond timescale. Our results clearly show that single-cycle terahertz pulses can be used to significantly modulate the nature of superionic conductors and could possibly serve as a basic tool for application in future electronic devices.

DOI: 10.1103/PhysRevLett.124.147401

Recent advances in ultrashort laser technology have enabled the control of carrier-envelope phases of few-cycle pulses, which play critical roles in nonperturbative, nonlinear phenomena [1–8]. Such studies provide possibilities for petahertz science with attosecond light fields, generation of high harmonics, and field-induced tunneling. However, most of these phenomena are dominated by the ultrafast electron dynamics of materials, and the nonperturbative responses of ions have rarely been investigated. This is because the greater the mass of ions compared to that of electrons, the more difficult it becomes to manipulate these ions over a substantial distance from their equilibrium position. In addition to electron motion, ionic motion is a key factor affecting the atomic arrangements in solids [9]. Thus, it is important to investigate the possibility of controlling the ionic motion in nonperturbative regimes using external light fields.

An intuitive consideration of ionic motion based on the electron–proton mass ratio ($m_p/m_e \approx 1840$) and electron-electron scattering time in femtoseconds (fs) suggests that the dynamics of ions should evolve on picosecond (ps) timescales corresponding to the terahertz frequency range. Therefore, intense phase-locked terahertz waves at sufficiently high field strengths could possibly be used to generate a nonperturbative ionic response, which may be useful for controlling material properties in future electro-ionic devices [10]. To demonstrate the field control of ionic motion, this Letter focuses on a superionic conductor in which the current is normally carried by cations in the periodic potential minima in the lattice. We show that a field-driven ionic motion is induced by applying an intense terahertz field, generating a macroscopic current that depends on the polarity of the applied terahertz field.

As Na^+ ion control is one of the key technologies for next-generation power sources, such as rechargeable rare-metal-free batteries [11–13], we investigate stoichiometric crystalline Na^+ β-alumina, which is a superionic conductor wherein Na^+ ions move in the two-dimensional space between the spinel layers perpendicular to the c axis [14]. At room temperature, the shape of the energy potential for Na^+ ion capture can be simply approximated using a cosine function in the ion propagation direction [14], enabling a simplified and intuitive analysis of the ion dynamics.

Figure 1 shows the schematic of the experimental setup used in this study. We used stoichiometric crystalline Na^+ β-alumina as the sample [14,15]. The dimensions of the sample are 23 μm (thickness, c-axis direction) $\times$1 mm (width) $\times$2 mm (electrode spacing). The intense terahertz field was generated using a tilted-pulse-front method via a $LiNbO_3$ prism [16,17]. The terahertz field strength was varied using a pair of wire-grid polarizers. The terahertz pulse was incident normal to the sample surface, and the polarization of the field was kept parallel to the direction of electrode spacing and perpendicular to the c axis. As the radius of the terahertz beam incident on the sample is 0.5 mm, nearly 40% of the sample was exposed to intense terahertz radiation. The applied terahertz field stimulated the trapped Na^+ ions at a laser repetition rate of 1 kHz, and the resultant terahertz-field-induced direct electric current was measured using an ammeter. The experiments were carried out under a nitrogen atmosphere at room temperature.

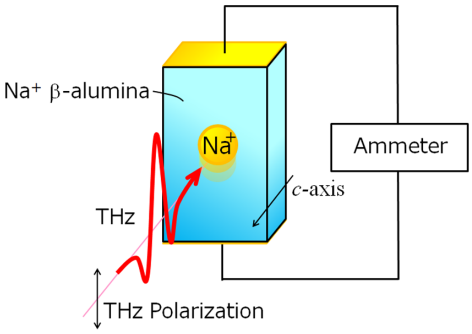

FIG. 1. Setup used for measuring the ionic current induced by the terahertz pulse. The induced macroscopic current is measured using an ammeter. The Na^+ ions in the sample move in the two-dimensional space between the spinel layers perpendicular to the c axis.

We applied a terahertz pulse with a peak field strength ranging from 15 to 300 kV/cm. Figure 2(a) shows the dependence of the terahertz-induced direct current on the peak terahertz field strength (E) in Na^+ β-alumina. Although the terahertz pulse carries no direct-current components, a terahertz-induced direct current is detected using the ammeter at a high electric field strength. The current is detected only above a threshold field of $|E| \approx 50$ kV/cm. The maximum current measured is approximately 2 pA, and more importantly, the sign of the current depends on the polarity of the terahertz field. This indicates that the current is neither induced by ionic diffusion nor by electron excitation; in fact, it originates from the direct flow of ions induced by the terahertz electric field. When $|E| < 50$ kV/cm, the Na^+ ions vibrate around the local potential minima, as the energy supplied by the terahertz pulse is not high enough to overcome the peak potential barrier [see the left portion of Fig. 2(b)]. Consequently, the Na^+ ions remain trapped and are immobile, and no current is induced. When $|E| >$ 50 kV/cm, the Na^+ ions become mobile, as their kinetic energy exceeds the barrier height [see the right portion of Fig. 2(b)]. In this case, the Na^+ ions move within the sample, inducing a detectable macroscopic current.

To elucidate the change in the ion dynamics observed in the terahertz-induced current measurements, we carried out field-dependent terahertz time-domain spectroscopy measurements. The generated terahertz field is incident on the sample, and the transmitted field is measured using an electro-optic (EO) sampling method [see the left portion of Fig. 3(a)]. Figure 3(b) shows the terahertz field dependence of the energy absorbance. With weak terahertz pulses, the absorption peak is clearly observed on the broad background at ~1.8 THz; this peak corresponds to the vibrational mode of the Na^+ ions oscillating at the bottom of the potential well at room temperature [14]. As the terahertz field strength increases, the peak drastically diminishes before finally vanishing at $E \approx 300$ kV/cm. To better understand this result, we plot the field dependences of the normalized

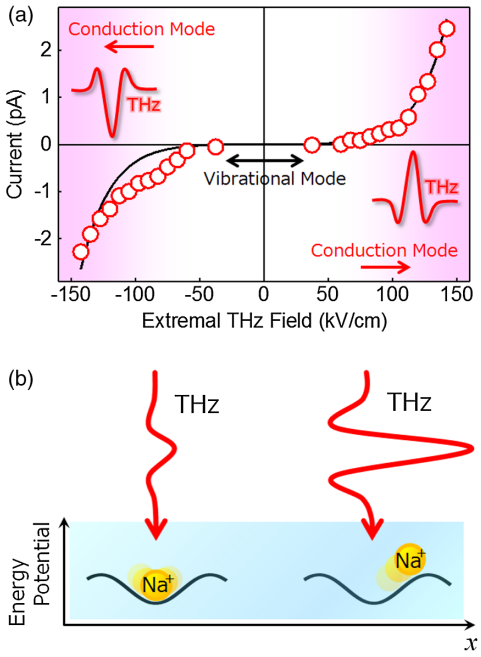

FIG. 2. Response of an ion in the sample under terahertz-field illumination. (a) Terahertz intensity dependence of the ionic current averaged 10^3 times, measured using an ammeter. The current direction changes based on the polarity of the terahertz field. The solid curve is the best fit of Eq. (1). (b) Configuration of the ion and local potential in real space for Na^+ β-alumina at room temperature. The left side of the figure shows the Na^+ ion in the vibrational mode under weak terahertz-field illumination, whereas the right side shows the ion in the conduction mode under intense terahertz-field illumination.

absorbance and center frequency associated with the Na^+ ion vibrations, as shown in Figs. 3(c) and 3(d), respectively. Here, to isolate the contribution of the vibrational mode, we performed the fitting using two Gaussian curves: one was used for evaluating the vibrational mode with a center frequency of approximately 1.8 THz, and the other was used for evaluating the broad background with a center frequency of ~1.2 THz. Although the origin of the background remains unclear, we found that neither the absorbance nor the center frequency of the mode at 1.2 THz depend on the terahertz field strength, implying that the background is independent of the terahertz-field-induced phenomena. The peak absorbance for fields greater than 150 kV/cm is almost ten times lower than that for a field of 38 kV/cm. As the peak absorbance is proportional to the density of the trapped Na^+ ions, this result implies that most of the Na^+ ions are promoted to the conduction mode when the peak terahertz field exceeds 150 kV/cm. Assuming that all the Na^+ ions are in the vibrational mode under a weak electric field of 38 kV/cm and in the conduction mode under a high electric field of 300 kV/cm, the terahertz-field-induced current is proportional to the fraction of Na^+ ions in the conduction mode multiplied by the terahertz field strength. Figure 3(c) shows the plot of the terahertz-induced current with respect to

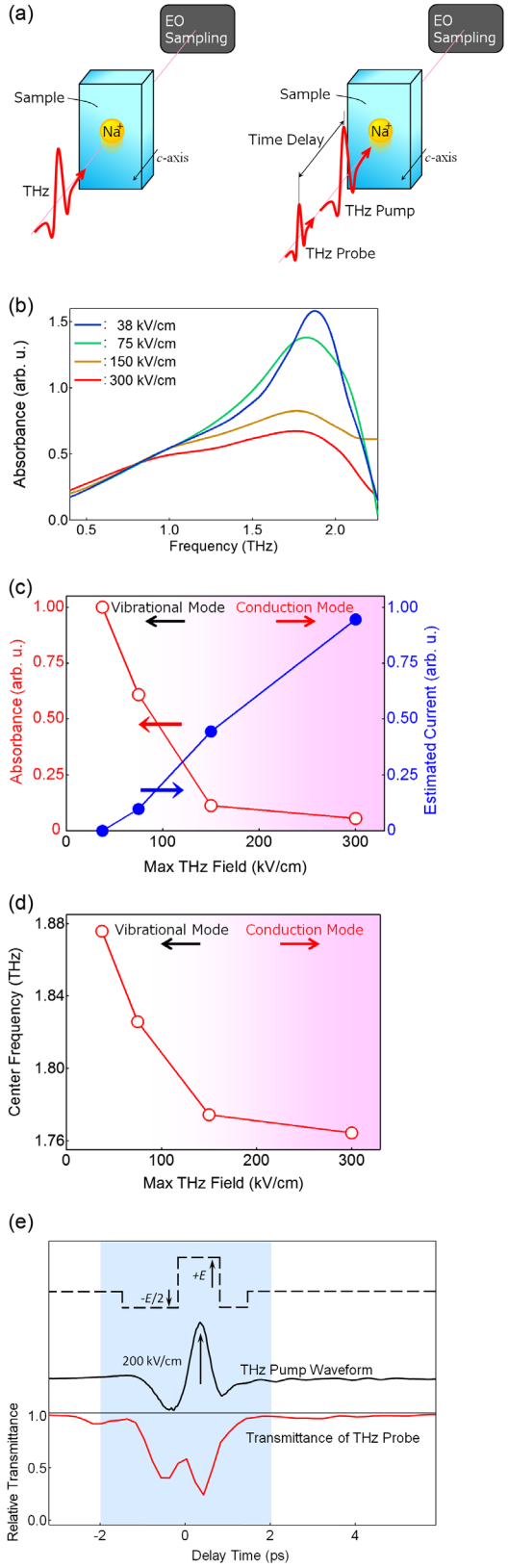

the change in the absorbance, indicating a strong correlation between these phenomena. In addition, a slight frequency softening of the absorption peak is observed [see Fig. 3(d)], which is expected as the shape of the energy potential has a smaller slope at high energies. From the spectral analyses shown in Figs. 3(c) and 3(d), the spectral change, shown in Fig. 3(b), provides a strong evidence for the terahertz-field-induced ionic motion. As the terahertz-induced current is also proportional to the distance traveled by the ions from their original positions, the total time during which the ions remain mobile is significant. To experimentally investigate the total time, we employed intense terahertz pump–terahertz probe spectroscopy [see the right portion of Fig. 3(a)]. The peak terahertz electric field of the probe beam is approximately 5 kV/cm, which is weak enough to avoid the stimulation of Na^+ ion motion. Figure 3(e) shows the time dependence of the transmittance intensity of the terahertz probe pulse averaged over a frequency range of 0.4–2.2 THz as a function of the pump-probe delay. The middle of the figure shows the terahertz pump waveform. As shown in this

FIG. 3. (a) Outline of the experimental setup of terahertz time-domain spectroscopy. The generated terahertz field is incident on the sample, and the transmitted field is measured using an electro-optic (EO) sampling method (left side). The terahertz pump–terahertz probe spectroscopy used in this study is shown on the right side of (a). The experiments shown in (a) are carried out under a nitrogen atmosphere at room temperature. (b) Terahertz intensity dependence of the absorbance for the sample. The peak at 1.8 THz corresponds to Na^+ ion vibrations; the peak vanishes as the terahertz field becomes more intense. (c) Terahertz intensity dependence of the normalized absorbance of Na^+ ions (red line and open circle). As the terahertz field becomes more intense, the absorbance decreases drastically, implying that the ions are trapped in their local potentials under weak terahertz fields, whereas they escape from their local potentials under intense terahertz fields. In other words, the motion of Na^+ ions changes from a vibrational mode to a conduction mode. The terahertz intensity dependence of the current obtained by an estimation stated in the main text is also shown in this figure (blue line with solid circles); the results are in good qualitative agreement with that shown in Fig. 2(a). (d) Terahertz intensity dependence of the center frequency of the Na^+ ion absorption. The center frequency decreases as the terahertz field becomes more intense. (e) Relative terahertz transmittance measured using intense terahertz pump–terahertz probe spectroscopy. The transmittance of the probe terahertz pulse decreases only when the sample is illuminated by an intense terahertz field (shaded area), implying that the ions move only when the pump terahertz field is incident on the sample. The scaled terahertz electric field with a square waveform used for the calculation is also shown.

figure, the transmittance decreases only when the electric field of the terahertz pump is sufficiently high regardless of the polarity of the terahertz pulse and recovers immediately (∼sub-ps timescale) following terahertz pump illumination. The lack of change in the transmittance with respect to the zero time suggests that the conductivity changes only when the terahertz pump is present and that the ions remain trapped in the absence of the field. From the above results, the mechanism involved in the current generation can be qualitatively understood as follows. In the absence of a terahertz field, the Na^+ ions are trapped in the periodic potential minima in the lattice. If the Na^+ ions are not given sufficient energy to overcome the potential barrier, the ions will vibrate at the bottom of the potential well, as shown in the left portion of Fig. 2(b), and no current will be detected. However, with a high terahertz field, the vibrational frequency decreases because of the anharmonicity brought on by the cosine shape of the energy potential. If the additional energy provided by the terahertz field is sufficient to overcome the potential barrier, the Na^+ ions will be transported until the supplied energy is relaxed. The net current can be detected using a conventional ammeter.

To understand the observed ion dynamics, we examined two simple simulation models: a standard transport model based on the equation of motion of Na^+ ions (Supplemental Material [18]) and a thermally excited transport model [25]. The former model can qualitatively explain the ion dynamics, particularly the time transient of the position in real space (Fig. 1S). However, this model predicts much higher field (∼30 MV/cm) for the delocalization of Na^+ ions than the experimentally observed depinning field (∼50 kV/cm), whose discrepancy might come from factors excluded from the model such as thermal activation of Na^+ ions and many-body effects. In the latter model, therefore, we introduce the thermally excited current driven by the terahertz electric field expressed by

$$I(E) = f_{\mathrm{rep}} \times \int Sn\beta q\Lambda\nu \exp\left(-\frac{V_0}{k_B T}\right) \times 2\sinh\left(\frac{\beta q\Lambda E(t)}{2k_B T}\right) dt, \quad (1)$$

where S (=1 mm × 23 μm) is the cross section of the sample, n (=1×10^{25} m^{-3} [26]) is the Na^+ ion density, β is the adjustable effective factor [27,28], $q = e(>0)$ is the charge on the Na^+ ions, Λ (=6.4 Å) is the potential period [14], ν (=1.8 THz) is the vibrational frequency of the Na^+ ions, V_0 (=0.5 eV) is the height of the potential barrier [14], k_B is the Boltzmann constant, T (=290 K) is the lattice temperature, and $E(t)$ is the applied electric field. The electric field modifies the height of the potential barrier by $-q(\Lambda/2)E$ [$+q(\Lambda/2)E$] for [against] the electric field, and resultantly, the mean velocity of the ion is given by $\Lambda\nu\exp(-V_0/k_BT) \times 2\sinh(q\Lambda E/2k_BT)$, where $\nu\exp(-V_0/k_BT)$ corresponds to the frequency factor that thermally climbs over the potential barrier. The effective parameter β modifies either the charge or the potential period, i.e., hopping length of the Na^+ ions. Here, we simply assume that the terahertz electric field has a positive and negative oscillatory square waveform with 3 ps as shown by a broken line in Fig. 3(e). By taking the square-shaped terahertz electric field with a repetition rate of 1 kHz ($f_{\mathrm{rep}} = 1$ kHz) into consideration, we could remove the direct-current components from our analysis and simply calculate the total current $I(E)$. By using the parameter value of $\beta = 62$, we could quantitatively reproduce the experimental data as shown by a solid curve in Fig. 2(a). The large value of β implies that either the charge or the hopping length is somewhat enhanced due to implicit factors such as collective and many-body effects. Despite the simplicity of our simulation models, most of the experimental results could be reproduced, and the models can provide useful insight into the underlying physics of ion dynamics in superionic conductors; the standard transport model based on the equation of motion provides the qualitative ionic dynamics in real space, while the thermally excited current model numerically reproduces the macroscopic ionic current induced by the applied terahertz electric field. The obtained experimental and simulation results strongly suggest that the ions in a superionic conductor can be driven nonperturbatively to induce a current and that the ions travel several nanometers on subpicosecond timescales.

In conclusion, we experimentally accelerated the ions in a Na^+ β-alumina superionic conductor by applying intense terahertz fields and measured the induced macroscopic direct current. Through terahertz time-domain spectroscopy measurements, we observed a reduction in the vibrational absorption because of the absence of vibrating ions. In addition, we implemented two simple analyses to understand the observed ion dynamics. By using the equation of motion of Na^+ ions, we could simulate ion movements in real space and clarified that the response of Na^+ ions to the terahertz field was due to a change in their dynamics from a vibrational mode to a conduction mode. By calculating the thermally excited current driven by the terahertz electric field, the terahertz-field-induced macroscopic current could be semi-quantitatively explained using the enhancement factor of β. Although a sophisticated theory to quantitatively explain the overall ion dynamics is still required, we believe that our finding—macroscopic current flow in a superionic conductor driven by single-cycle terahertz pulses—may pave the way for future ultrafast ionics.

This work was supported in part by the Grants-in-Aid for Scientific Research (KAKENHI, No. 17H06124, No. 18H04288, and No. 19K03701) from the Japan Society for the Promotion of Science (JSPS). The research at MIT was supported in part by U.S. NSF Grant No. CHE-1665383.

*minami@tokushima-u.ac.jp

[1] P. B. Corkum and F. Krausz, Nat. Phys. **3**, 381 (2007).
[2] M. Krüger, M. Schenk, and P. Hommelhoff, Nature (London) **475**, 78 (2011).
[3] A. Schiffrin *et al.*, Nature (London) **493**, 70 (2013).
[4] F. Krausz and M. I. Stockman, Nat. Photonics **8**, 205 (2014).
[5] L. Wimmer, G. Herink, D. R. Solli, S. V. Yalunin, K. E. Echternkamp, and C. Ropers, Nat. Phys. **10**, 432 (2014).
[6] T. Rybka, M. Ludwig, M. F. Schmalz, V. Knittel, D. Brida, and A. Leitenstorfer, Nat. Photonics **10**, 667 (2016).
[7] A. V. Kolobov, P. Fons, A. I. Frenkel, A. L. Ankudinov, J. Tominaga, and T. Uruga, Nat. Mater. **3**, 703 (2004).
[8] K. Yoshioka, I. Katayama, Y. Minami, M. Kitajima, S. Yoshida, H. Shigekawa, and J. Takeda, Nat. Photonics **10**, 762 (2016).
[9] Y. Kato, S. Hori, T. Saito, K. Suzuki, M. Hirayama, A. Mitsui, M. Yonemura, H. Iba, and R. Kanno, Nat. Energy **1**, 16030 (2016).
[10] B. N. Pal, B. M. Dhar, K. C. See, and H. E. Katz, Nat. Mater. **8**, 898 (2009).
[11] B. L. Ellis, W. R. M. Makahnouk, Y. Makimura, K. Toghill, and L. F. Nazar, Nat. Mater. **6**, 749 (2007).
[12] N. Yabuuchi, M. Kajiyama, J. Iwatate, H. Nishikawa, S. Hitomi, R. Okuyama, R. Usui, Y. Yamada, and S. Komaba, Nat. Mater. **11**, 512 (2012).
[13] X. Wang, S. Kajiyama, H. Iinuma, E. Hosono, S. Oro, I. Moriguchi, M. Okubo, and A. Yamada, Nat. Commun. **6**, 6544 (2015).
[14] G. Lucazeau, Solid State Ionics **8**, 1 (1983).
[15] J. R. Walker and C. R. A. Catlow, J. Phys. C **15**, 6151 (1982).
[16] J. Hebling, G. Almási, I. Z. Kozma, and J. Kuhl, Opt. Express **10**, 1161 (2002).
[17] H. Hirori, A. Doi, F. Blanchard, and K. Tanaka, Appl. Phys. Lett. **98**, 091106 (2011).
[18] See Supplemental Material at http://link.aps.org/supplemental/10.1103/PhysRevLett.124.147401 for details of the ion dynamics, particularly the time transient of the position in real space, and the spectrum change induced by intense terahertz fields, which includes Refs. [19–24].
[19] P. Colomban and G. Lucazeau, J. Chem. Phys. **72**, 1213 (1980).
[20] W. Kuehn, P. Gaal, K. Reimann, M. Woerner, T. Elsaesser, and R. Hey, Phys. Rev. Lett. **104**, 146602 (2010).
[21] T. Shih, K. Reimann, M. Woerner, T. Elsaesser, I. Waldmüller, A. Knorr, R. Hey, and K. H. Ploog, Phys. Rev. B **72**, 195338 (2005).
[22] Y. Minami, K. Araki, T. D. Dao, T. Nagao, M. Kitajima, J. Takeda, and I. Katayama, Sci. Rep. **5**, 15870 (2015).
[23] U. Strom, P. C. Taylor, S. G. Bishop, T. L. Reinecke, and K. L. Ngai, Phys. Rev. B **13**, 3329 (1976).
[24] A. S. Barker, Jr., J. A. Ditzenberger, and J. P. Remeika, Phys. Rev. B **14**, 4254 (1976).
[25] N. F. Mott and R. W. Gurney, *Electronic Processes in Ionic Crystals* (Dover, New York, 1948), Chap. II.
[26] K. L. Ngai and U. Strom, Phys. Rev. B **38**, 10350 (1988).
[27] I. Katayama, H. Aoki, J. Takeda, H. Shimosato, M. Ashida, R. Kinjo, I. Kawayama, M. Tonouchi, M. Nagai, and K. Tanaka, Phys. Rev. Lett. **108**, 097401 (2012).
[28] B. E. Knighton, R. T. Hardy, C. L. Johnson, L. M. Rawlings, J. T. Woolley, C. Calderon, A. Urrea, and J. A. Johnson, J. Appl. Phys. **125**, 144101 (2019).

Supplementary Material: Macroscopic Ionic Flow in a Superionic Conductor Na^+ β-Alumina Driven by Single-Cycle Terahertz Pulses

Yasuo Minami,[1,2,*] Benjamin Ofori-Okai,[3] Prasahnt Sivarajah,[3] Ikufumi Katayama,[2] Jun Takeda,[2] Keith A. Nelson,[3] and Tohru Suemoto[4]

[1]*Department of Industrial and Social Sciences, Tokushima University, Tokushima 770-8506, Japan*
[2]*Department of Physics, Faculty of Engineering Science, Yokohama National University, Yokohama 240-8501, Japan*
[3]*Department of Chemistry, Massachusetts Institute of Technology, Massachusetts 02139, USA*
[4]*Toyota Physical and Chemical Research Institute, Nagakute, Aichi 480-1192, Japan*

To numerically understand the ion dynamics, particularly the time transient of the position in real space, we simulated the movement of Na^+ ions induced by the terahertz field transients in real space based on the simple equation of motion expressed as follows.

$$\frac{d}{dt}p(t) + \Gamma p(t) + \mathrm{grad}V = qE_{\mathrm{tr}}(t), \tag{S1}$$

where $p(t)$ is the momentum of the ions, Γ is the damping constant, and V can be expressed using a periodical potential model, $V = \frac{V_0}{2}\left(1 - \cos\frac{2\pi x}{\Lambda}\right)$ [19]. V_0 is the amplitude of the potential barrier [14] and is set to 0.5 eV with a standard deviation of 0.05 eV. Λ (= 6.4 Å) is the potential period [14], $q = e(> 0)$ is the charge on the Na^+ ions, and $E_{\mathrm{tr}}(t) = E_{\mathrm{in}}(t) + E_{\mathrm{em}}(t)$ is the electric field transmitted through the sample. Here, $E_{\mathrm{in}}(t)$ represents the electric field applied to the sample, whereas $E_{\mathrm{em}}(t)$ represents the electric field emitted from the sample including the ionic-current-induced electric field [20]. As the thickness of the sample (l = 23 μm) is lower than the wavelength of the applied terahertz field ($\lambda \approx 600$ μm), all the ions in the sample experience the same driving field $E_{\mathrm{tr}}(t)$ [21]. Based on a thin-film approximation for the sample, the driving field is given by the induced current as follows [22].

$$E_{\mathrm{tr}}(t) = \frac{1}{n_N + 1}\left[2E_{\mathrm{in}}(t) - Z_0 j(t) l\right], \tag{S2}$$

where n_N ($\approx$ 1) is the refractive index of nitrogen gas, Z_0 ($\approx$ 377 Ω) is the impedance of free space, and $j(t)$ is the current density in Na^+ β-alumina. The current density $j(t)$ is expressed as $j(t) = nqp(t)/m$, where n is the Na^+ ion density, and m is the mass of a bare Na^+ ion. Therefore, Eq. (S1) can be rewritten as follows.

$$\frac{d}{dt}p(t) + \Gamma p(t) + \mathrm{grad}V = q\frac{1}{2}\left[2E_{\mathrm{in}}(t) - Z_0 nq\frac{p(t)}{m}l\right]. \tag{S3}$$

The values used for the simulation are $\Gamma = 1 \times 10^{10}$ s^{-1} at approximately 0.5 THz [23], $n = 1 \times 10^{25}$ m^{-3} [26], and $m = 3.8 \times 10^{-26}$ kg [23].

Figure S1 shows the trajectories of the position of an ion under weak and intense terahertz-field illuminations, respectively. With a weak terahertz pulse, the ion remains at the initial site and vibrates at the bottom of the potential well. With an intense terahertz pulse, the ion becomes mobile and travels to another site on a sub-picosecond timescale until the field strength falls below the threshold value (i.e., the depin-

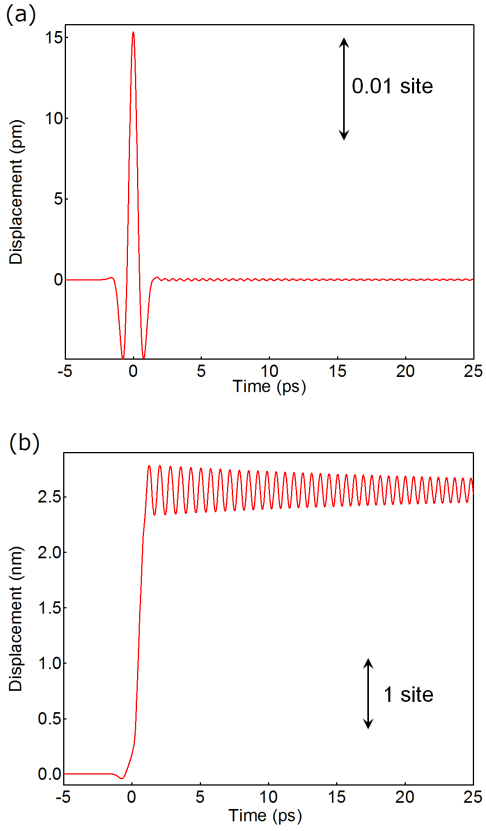

FIG. S1. Simulated Na^+ ion dynamics. (a) Time transient for ion displacement under a weak terahertz field. The Na^+ ion vibrates in the initial site. Note that the unit of the left axis is pm. (b) Time transient of an ion position under an intense terahertz field. The Na^+ ion moves to another site on a sub-picosecond timescale. After the movement, the Na^+ ion vibrates in the site. Note that the unit of the left axis is nm.

* minami@tokushima-u.ac.jp

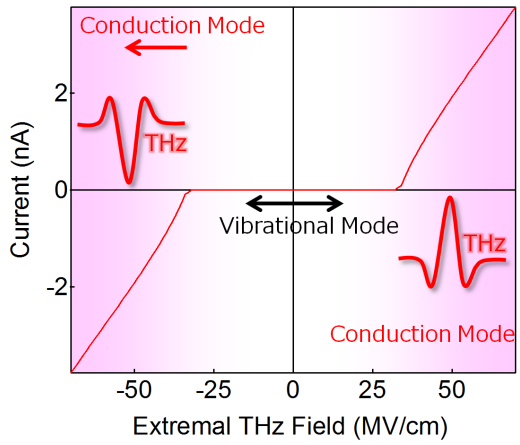

FIG. S2. Simulated terahertz intensity dependence of the ionic current, which is in qualitative agreement with the experimentally obtained results [see Fig. 2(a)].

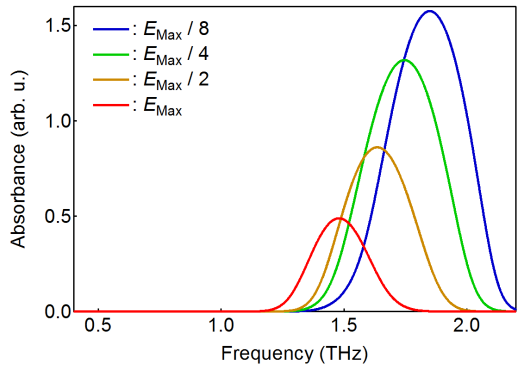

FIG. S3. Simulated absorbance under different terahertz fields; the results are in good agreement with the experimentally obtained spectra. For comparison with the experimental result shown in Fig. 3(b), the absorbance is appropriately scaled. In this simulation, the nonuniformity for each ion motion is considered. As shown in the figure, the vibrational spectra diminish as the terahertz intensity increases.

ning value), at which point the ion is trapped and vibrates at the destination site. From the calculated travel distances of the ions, we can estimate the induced current. Figure S2 shows the obtained electric field dependence of the current. As shown in this figure, the simulation qualitatively reproduces the electric field dependence of the current; the current nonlinearly increases with the electric field above the depinning electric field [see Fig. 2]. However, the calculated depinning electric field (~ 30 MV/cm) is much larger than that observed from the experiment. The significant discrepancy between the simulation and experimental results is most likely due to unhandled factors in this model, such as the thermal excitation which contributes to the ion movement and resultant suppression of the net potential barrier, the many-body effect originating from Coulomb interactions between Na^+ ions, the subsequent modification of the local potential from the cosinusoidal shape, the modification of the potential shape induced by the terahertz field, and so on [24]. The Coulomb force between the Na^+ ions facilitates the motion of the Na^+ ions over the potential barrier, which may lead to a lower threshold depinning electric field as observed in the experiment. Although the absolute values differ, the overall trend is in good agreement with the experimental result shown in Fig. 2(a). We can also calculate the absorbance by considering the inhomogeneous broadening of the vibrational mode, as shown in Fig. S3. The simulations show a reduction in the ion absorption peak at 1.8 THz with the increase in the terahertz electric field; this is in good agreement with the experimental results as shown in Fig. 3(d). The difference in the degree of frequency shift could be due to the difference between the theoretical energy potential shape and the actual energy potential shape of Na^+ β-alumina. Despite the simplicity of our simulation model, most of the experimental results could be qualitatively reproduced, and the model can provide useful insight into the underlying physics of ion dynamics in superionic conductors. Especially, we could demonstrate the traveling times of the ions on a sub-picosecond timescale, which is useful for future ultrafast ionics.